The functional and pathogenic consequences of fibrinogen on human oligodendroglia

Gabriela J. Blaszczyk MSc[1], Chao Weng MD[1,2], Abdulshakour Mohammadina PhD[1], Qiao Ling Cui MD PhD[1], Arianna Giurleo BSc[1], Adam M.R. Groh MSc[1], Chloe Plouffe BSc[1], Julien Sirois PhD[3], Valerio E. C. Piscopo PhD[3], Moein Yaqbi PhD[1], Asad Taqvi BSc[1], Jeffery A. Hall MD[4], Roy W.R. Dudley MD[5], Myriam Srour MD[6], Stephanie E J Zandee PhD[7], Wendy Klement MSc[7], Sandra Larouche DCS[7], Alexandre Prat MD PhD[7], Thomas M. Durcan PhD[3], Jo Anne Stratton PhD[1], Jack P. Antel MD[1], G. R. Wayne Moore MD[1,8,9].

Author Affiliations:

1. Neuroimmunology Unit, Montreal Neurological Institute and Department of Neurology and Neurosurgery, McGill University, Montreal H3A 2B4, Canada.
2. Department of Neurology, Renmin Hospital of Wuhan University, Wuhan, Hubei 430060, P.R. China.
3. Early Drug Discovery Unit, Montreal Neurological Institute-Hospital, McGill University, Montreal H3A 2B4, Canada.
4. Department of Neurosurgery, McGill University Health Centre and Department of Neurology and Neurosurgery, Montreal H3A 2B4, Canada.
5. Department of Pediatric Neurosurgery, Montreal Children's Hospital, Montreal H4A 3J1, Canada.
6. Division of Pediatric Neurology, Montreal Children's Hospital, Montreal H3A 2B4, Canada.
7. Centre de Recherche Hospitalier de l'Université de Montréal, Montreal H2X 0A9, QC, Canada.
8. Department of Pathology and Laboratory Medicine, University of British Columbia; International Collaboration on Repair Discoveries (ICORD), Vancouver V5Z 1M9, BC, Canada.
9. Division of BioMedical Sciences, Memorial University of Newfoundland, St. John's A1C 5S7, NL, Canada

Corresponding Author: Dr. Wayne Moore, wayne.moore@mcgill.ca

Running Title: Fibrinogen effect on human oligodendroglia

Characters (title): 72
Characters (running title): 38
Word count:
Abstract: 250 words
Introduction: 464 words
Discussion: 1157 words
Total word count: 4407 words

Number of figures: 6 main text, 2 supplementary, 3 supplementary tables

Abstract

Objective: Multiple sclerosis is an inflammatory demyelinating disorder associated with blood-brain-barrier breakdown, where myelin repair is reduced and ultimately fails. Our aim was to investigate the effect of a systemically circulating molecule fibrinogen, which is abnormally present in the central nervous system as a result of blood-brain barrier breakdown on human oligodendrocyte lineage cells.

Methods: In situ immunofluorescence was performed using anti-fibrinogen and anti-SOX10 antibodies. Mature oligodendrocytes and late progenitors were derived from brain tissue from pediatric and adult donors. Early progenitors were generated from human induced pluripotent stem cells. Following fibrinogen addition to each of these cultures, cell viability and functional capacity was evaluated. Downstream signalling following fibrinogen exposure was confirmed by immunofluorescence microscopy and bulk RNA sequencing.

Results: In situ studies showed fibrinogen on SOX10-positive oligodendrocytes in multiple sclerosis, both in plaques and normal-appearing white matter, and white matter in amyotrophic lateral sclerosis. In response to in vitro exposure to fibrinogen, mature oligodendrocytes showed increased ensheathment capacity and upregulation of lipid synthesis, whereas pediatric-age late oligodendrocyte precursors showed a decrease. Early precursors were unable to differentiate but expressed astrocytic markers and increased proliferation. Fibrinogen-exposed cells show bone morphogenetic protein signalling, more prominently in mature oligodendrocytes.

Interpretation: We demonstrate that fibrinogen is deposited on oligodendrocytes in multiple sclerosis and has distinct functional consequences dependent on cell lineage stage. Our findings derived using human OL lineage cells suggest fibrinogen may be beneficial for myelin maintenance by mature oligodendrocytes, while preventing earlier lineage cells from differentiating and repairing multiple sclerosis lesions.

1. Introduction

Multiple Sclerosis (MS) is an autoimmune disease of the central nervous system (CNS) characterized clinically by an initial relapse-remitting stage that can evolve over years into a progressive disease course. Initial lesion formation is attributed to targeting and injury of oligodendrocytes (OL) and their myelin membranes by infiltrating immune cells and their products[1] . In the initial lesions, OL cell bodies are relatively preserved with retraction of their cell processes[2], but they eventually succumb[3]. Failure of myelin repair is attributed to both the susceptibility to injury[4] and reduced ability of oligodendrocyte precursor cells (OPC) to differentiate into mature OLs [5].

Potential contributors to the injury and repair responses are blood-derived factors that may access the CNS due to the breakdown of the blood-brain barrier (BBB)[6]. Fibrinogen is a circulating blood clotting factor composed of polypeptide chains which have polymerization sites for clot formation [7], and various domains known to be involved in stimulation of multiple cell types [8]. Fibrinogen has been detected in the borders of chronic active white matter plaques [9] and leakage into diffusely abnormal white matter (DAWM) has also been described [10]. It has also been found in MS motor cortex, where its presence significantly correlated with reduced neuronal density[11], implicating its direct role in cellular damage. In MS, fibrinogen has been found at the cellular level in astrocytes[12, 13]; neuronal axons[10], and macrophages[12]. Moreover, plasma levels of fibrinogen are elevated in MS relapses [14]; its role in MS pathogenesis has been linked to its function in the coagulation cascade and as a pro-inflammatory agent[15]. The role of fibrinogen in MS and autoimmune disorders of the CNS has been extensively studied by Akassoglou and colleagues [16], and experimental studies in her laboratory have shown that fibrinogen can inhibit the differentiation of rodent OPCs into myelinating oligodendrocytes, primarily mediated via bone morphogenetic protein (BMP) signaling [17].

The objectives of our study were to extend insights into the effects of fibrinogen on human OLs by means of in situ studies demonstrating its presence on OLs in MS tissues and in vitro studies showing its functional effects on OLs throughout their lineage. We employed primary human mature OLs (O4+A2B5-) and late lineage cells (O4+A2B5+) [18, 19] derived from non-MS surgically resected tissue samples together with early-stage progenitor cells derived from human induced pluripotential stem cells (iPSCs), as such primary cells cannot currently be derived from available human sources. Primary cell studies were also considered in context of the donor age, as we previously reported that ensheathment capacity, as determined using cultures with synthetic nanofibers, and susceptibility to injury were donor age dependent [20]. For iPSC studies, we also employed a previously characterized line expressing a reporter gene under the SOX10 promoter, where the degree of SOX10-mOrange expression correlated with differentiation stage of the cells[21].

2. Materials and Methods

Human multiple sclerosis brain tissue

This study was ethically approved by the Institutional Review Board of the McGill University Faculty of Medicine and tissues from the Centre Hospitalier de l'Université de Montréal (CHUM) were obtained by a Material Transfer Agreement between CHUM and McGill University. Human

brain tissue was obtained from patients diagnosed MS diagnosis according to the revised 2010 McDonald's criteria[22]. Tissue samples were collected from one amyotrophic lateral sclerosis (ALS) patient and three MS patients (Table S1) with full ethical approval (BH07.001, Nagano 20.332-YP) and informed consent as approved by the local ethics committee. Autopsy samples were preserved, and lesions classified [23] using Luxol Fast Blue-Haematoxylin and Eosin (LFB-HE) staining as previously published [24,25].

Antibodies

Antibodies used in this study are listed in Table S3.

In situ immunohistochemistry

In situ immunohistochemistry was done on frozen human brain tissue previously fixed in acetone. Primary antibodies used were SOX10 (R&D systems, Oakville ON) as an oligodendroglial lineage marker and fibrinogen (Agilent, Santa Clara CA) (see supplementary data for detailed protocol and reagents). The slides were examined for cellular co-localization of SOX-10 and fibrinogen under a Zeiss Axio Observer epifluorecence microscope (Carl Zeiss Canada, Toronto, ON). The total number of SOX10-positive cells in the imaged area within an MS plaque, in adjacent normal appearing white matter (NAWM) and in ALS white matter was determined by the QuPath Bioimage analysis software [26]. The number of SOX10-positive cells that were also fibrinogen-positive in that area was determined by the cell detection command and expressed as a percentage of the total number of SOX10-positive cells.

Human primary cell isolation and culture

Studies were conducted on OLs derived from pediatric (2.5 -18 years) and adult (26 - 65 years) tissue samples collected from patients undergoing surgery. The use of adult tissues was approved by the Montreal Neurological Institute Neurosciences Research Ethics Board and the use of paediatric tissues by the Montreal Children's Hospital Research Ethics Board. As previously described [19, 20] , samples were dissociated by trypsin digestion and subjected to Percoll gradient (Sigma, Oakville, ON) separation. To enrich progenitor populations, MACS magnetic beads selection against the cell surface marker A2B5 (Miltenyi Biotec, Auburn, CA) was performed following cell isolation, and positive and negative fractions were cultured. A2B5+ and A2B5- cells (30,000 cells per well) were plated into 96 well poly-L-lysine and extracellular matrix-coated plates (Thermo Fisher Scientific, Missisauga ON) in the same defined medium containing DMEM/F12+ N1 medium (Sigma, Oakville, ON) supplemented with B27 (Life Technologies, Grand Island, NY). Cells were treated with plasminogen-depleted fibrinogen (Millipore Sigma, Burlington MA, 341578, 80ug/ml to 4mg/ml) for 6 days. The cell viability was determined by live staining with propidium iodide (PI, Thermo Fisher Scientific, Missisauga, ON).

Nanofiber ensheathment cultures

Aliquots of A2B5+ and A2B5- cells were plated in multi-well aligned poly-L lactide nanofiber plates (The Electrospinning Company Ltd., Didcot, Oxfordshire, UK) (10,000 cells per microwell) and treated with fibrinogen in DMEM/F12+ N1 medium supplemented with B27 (Life Technologies, Grand Island, NY) and T3 (Sigma-Aldrich, Oakville, ON) for two weeks. Cell cultures were immunolabelled with O4 antibody diluted 1:200 (R&D Systems, Oakville, ON, MAB1326) followed by corresponding secondary antibodies (1:400) conjugated with Alexa Fluor

647 (Thermo Fisher Scientific, Missisauga ON). To determine the percentage of O4+ cells ensheathing a nanofiber in a culture, a blinded rater counted individual O4+ cells whose nanofibre-ensheathing processes could be identified as being connected to their cell bodies identified by Hoechst 33342 (Thermo Fisher Scientific, Missisauga, ON) staining of nuclei. Ensheathed processes were recognized by their straight alignment with underlying nanofibers and increased thickness of the segments (Figure 2 F). Cells were assigned as ensheathing (one or more segments) or not and counted by the Plugin Cell Counter ImageJ program.

Human iPSC culture and OPC differentiation

iPSC-derived OL lineage cells were differentiated according to a recently published protocol [21]. The use of iPSCs and stem cells in this research was approved by the McGill University Health Centre Research Ethics Board (DURCAN_IPSC/2019–5374). Briefly, from healthy control iPSC lines as well as the SOX10-mOrange reporter line [21] generated at the Montreal Neurological Institute's (MNI) Early Drug Discovery Unit (EDDU) (Table S2), early OL-lineage progenitors were generated, and plated on poly-L-ornithine (Sigma-Aldrich, Oakville ON)/ laminin (Invitrogen, Waltham MA) coated culture vessels. Post day 75 *in vitro*, to passage, media was removed and TrypLE (Thermo-Fisher, Missisauga, ON) was added for 30 mins at 37°C. Cells are counted and replated, for up to a maximum of four passages. For differentiation, a commercially available kit consisting of basal medium and growth serum (ScienCell Research Laboratories, Carlsbad, CA) was used for 10 days, followed by addition of insulin-like growth factor-1 (Peprotech, Rocky Hill, NJ) and T3 (Sigma-Aldrich, Oakville, ON) for the following 11 days to reach a majority of OL-lineage cells at a total of 21 days. Cells were treated with plasminogen-depleted fibrinogen (Millipore Sigma, Burlington MA, 341578, 2.5 mg/ml) for 4 days prior to fixation (days 18-21 of differentiation). The cell viability was determined by live staining with propidium iodide (PI, Thermo Fisher Scientific, Missisauga, ON), differentiation capacity was determined by live staining with O4 (R&D Systems, Oakville ON, MAB1326) as described above. Proliferation was determined by staining with Ki67 (Invitrogen, Waltham MA, 14-5698-82), post-fixation and permeabilization according to manufacturer instructions. Secondary antibody was applied the following day as described above.

Signaling assessment

Primary human OLs and iPSC-derived OPCs following 21 days of differentiation were treated with molecules to induce signaling for 2 hours. The following concentrations were applied: plasminogen-depleted fibrinogen (Millipore Sigma, Burlington MA, 341578, 2.5 mg/ml), recombinant human BMP4 (Peprotech, Rocky Hill NJ, 50 ng/mL), BMP4-inhibitor 4-[6-(4-Isopropoxyphenyl)pyrazolo[1,5-a]pyrimidin-3-yl]quinoline (DMH1) (Selleck Chemicals, Houston TX, 2 uM). Post-fixation, cells were permeabilized with 100% cold methanol and stained with anti-pSMAD1/5/9 (Cell Signaling Technology, Danvers MA, 13820S) at a 1:50 dilution, and secondary antibodies (Alexa Fluor 488, 555 or 647; Invitrogen, Waltham MA) diluted to 1:400 were added the following day.

Immunofluorescence Analysis

To count cell numbers: Plates were imaged with a 10X objective using a Zeiss Axio Observer fluorescence microscope (Carl Zeiss Canada, Toronto) or the ImageXpress (Molecular Devices, San Jose, CA) high-content imaging platform following staining for O4, PI or Ki67. Cells were

counted by a blinded individual using the ImageJ software or automatically using the ImageXpress software.
To measure MFI: images were acquired on a Zeiss Axio Observer fluorescence microscope (Carl Zeiss Canada, Toronto, ON) at 20X objective or the Zeiss LSM 900 confocal microscope at 20X objective. For pSMAD1/5/9 nuclear intensity, nuclei of O4+ cells were selected by a blinded individual on the ImageJ software and the mean grey value of the pSMAD1/5/9 channel was recorded.
To record pSMAD localization: following image acquisition at the 20X objective, localization of pSMAD1/5/9 on O4+ cells was assessed by a blinded individual based on four criteria: no signal, cytoplasm only, nucleus and cytoplasm, nuclear only. 20-25 cells were counted for each replicate.

FACS Sorting and Flow Cytometry
For the iPSC-reporter line, cells were collected from the culture vessel using TrypLE (Thermo-Fisher, Missisauga ON) added for 30 mins at 37°C. The cells were passed through a 40µM mesh to ensure a single cell suspension. Following resuspension in PBS (Wisent, Saint-Jean-Baptiste, QC), the cells were counted using the Attune flow cytometer (Thermo-Fisher Scientific, Missisauga ON). Sorting was based on reporter intensity using the previously described protocol [21], with the aria fusion cell sorter (BD Biosciences, Franklin Lakes NJ). For phenotyping, cells were stained for viability using the LIVE/DEAD cell viability kit (Invitrogen, Waltham MA, L34957) according to manufacturer instructions. Then, cells were blocked using an FcX blocker (BioLegend, San Diego CA, 422302) and stained with pre-conjugated antibodies (O4-APC, Miltenyi, Auburn CA, 130-119-982; CD49f-PE-Dazzle, BioLegend, San Diego CA, #313626) for 30 minutes. Samples were acquired on the Attune flow cytometer (Thermo-Fisher Scientific, Missisauga ON), and data analyzed using the FlowJo software (Ashland, OR).

Bulk RNAseq preparation and analysis
Three subsequent passages of FACS-sorted SOX10-mOrange cells were collected as replicates, and primary cells from two different donors (53 yr, 58 yr) were collected as replicates following treatment with plasminogen-depleted fibrinogen (Millipore Sigma, Burlington MA, 2.5 mg/ml)for four and two days, respectively. Treated cells were collected and RNA was extracted according to the Qiagen (Hilden, Germany) RNA-mini kit or Norgen (Thorold, ON) single cell RNA purification kit.

Library preparation, sequencing, quality check, alignment, quantification of raw read counts: Library preparation, sequencing, quality check, alignment, quantification of raw read counts, and normalization of read counts were performed using the same methods described in Mohammadnia et al. (2024) [27].

Analysis of RNA-seq data from human primary oligodendrocytes: Due to the high level of patient heterogeneity, samples were analyzed in a pairwise manner as described in Mohammadnia et al. (2024) [27].

Analysis of RNA-seq data from iPSC-differentiated cells: As these samples did not exhibit significant heterogeneity and the lack of pair information for samples, we used DESeq2 for differential gene expression analysis following the methodology outlined in Pernin et al. (2024) [28, 29]. Significantly differentially expressed genes were identified using a threshold of log2 fold change > 1 and a p-value cutoff of < 0.05.

Heatmaps were generated following hierarchical clustering using the "Hierarchical Clustering Image" function in GenePattern (v3.9.11). Gene clustering was performed using Pearson correlation, and normalized values were transformed using a log transformation. Finally, row normalization was applied for the final visualization [30]. Single-sample Gene Set Enrichment Analysis (ssGSEA) was performed using the same method described in Mohammadnia et al. (2024) [27]. However, the signatures used in this analysis were BMP4 target genes extracted from the weighted matrix of ligand-target interactions in NichNet [31]. We selected target genes based on their weighted values, specifically those with a weight > 0.1 (n = 107 genes).

Single-cell RNA-seq analysis: All single-cell RNA-seq analyses were performed using the same pipeline employed in our previous publication[28] on the same Jakel et al. (2019) study [32].

Statistical analysis

Statistical analyses were performed using Excel or GraphPad Prism software. Cell culture studies were performed with at least three individual replicates per experiment (see figure legends for details). For iPSC-studies, three cell lines were used which contributed to values on graphs, and subsequent passages were used as biological replicates. Bars on graphs indicate means ±SEM. Student's t-test was used for comparisons between two groups. P-values <0.05 were considered statistically significant.

3. Results

Fibrinogen is deposited on OL-lineage cells in the MS brain

Tissue sections of brain were co-immunostained to detect SOX10 as a marker of OL lineage cells[33] and fibrinogen. We noted that fibrinogen was found on SOX10-positive oligodendroglia in MS lesions, the adjacent white matter, and in ALS white matter (Fig. 1A). This was quantitated in all areas, and there was great variability in the numbers of SOX10+/Fibrinogen+ cells (Fig. 1B). Given this co-localization in the MS brain, we then proceeded to evaluate the direct effect of fibrinogen on oligodendroglia *in vitro*.

Human primary OLs have an age and maturation-dependent functional response to fibrinogen

Dissociated OL cultures, comprised of 95 % mature OLs[20], were treated with fibrinogen. We observed no significant effect on cell viability (Fig. 2A) when fibrinogen was added over an 80ug/ml to 4mg/ml concentration range for 6 days. To determine a functional effect on OLs, we assessed their capacity to ensheath poly-L-lactide nanofibers. We separated pre-myelinating OLs (A2B5+) from mature OLs (A2B5-) to determine the relation of lineage maturity and donor age. In parallel with previous findings [20], pediatric-derived cells had an overall higher ensheathment capacity than adult cells (Fig. 2 D-E). In the presence of fibrinogen, we observed an increased capacity in adult-derived mature OLs (A2B5-) ($p < 0.05$) but no effect on adult A2B5+ cells (Fig. 2B). For pediatric donor cells, we observed a significant decrease in ensheathing A2B5+ cells ($p < 0.05$) but not mature OLs (A2B5-) in comparison to the age-matched untreated controls (Fig. 2C). Figures 2D-E shows the overall age-related effect of fibrinogen on mature (A2B5-) cells (Fig. 2E) and immature (A2B5+) cells (Fig. 2D), with representative images (Fig. 2F), indicating that fibrinogen has its most apparent positive effect on the older adult donors. Bulk RNAseq analysis of adult OLs shows upregulation of lipid metabolism pathways, including cholesterol synthesis, (Fig. 2G-H) consistent with this beneficial effect of fibrinogen on ensheathment by adult OLs.

Fibrinogen inhibits the differentiation of human OPCs

Since, as stated, we cannot isolate early OPCs from our surgical samples, we generated early OL-lineage cells from iPSCs, including a previously described human iPSC reporter line (SOX10mO) [21] where fluorescence intensity of the reporter correlates to the overall maturity of the cells. Fibrinogen treatment of early lineage cells, had no significant effect on OPC viability (Fig. 3A). Fibrinogen did significantly reduce the proportion of O4+ OPCs (Fig. 3B) as measured by immunofluorescence. To assess the effect of fibrinogen on overall differentiation into the OL lineage, we assessed level of expression of mOrange in our SOX10mO reporter line. As shown in Fig. 3C, placing these cells in differentiation media results in increased mOrange expression with a reduced proportion of undifferentiated (SOX10-neg) cells. Addition of fibrinogen resulted in an increase proportion of SOX10-med cells. We used the astrocyte-specific marker CD49f [34] to follow-up on the observation by Petersen et al. [17] that that fibrinogen diverts the differentiation of primary post-natal rodent derived OPCs towards the astrocyte lineage. We observed that the overall decrease in O4+ cells was associated with a significant ($p < 0.05$, t-test) increase in proportion of O4-CD49f+ cells and O4+CF49f+ cells following fibrinogen exposure (Fig. 3D, E). The latter hybrid OPCs retained the expression of our reporter (Fig. S1). To explore the molecular response of our medium level SOX10-mOrange cells, they were FACS-selected as previously described[21]. Bulk RNAseq analysis indicates that an overall decrease in signalling and differentiation occurring in these early OL-lineage cells, alongside significant upregulation of cell-cycle pathways (Fig. 3G-I), confirmed by Ki67 staining (Fig. S2). The latter would account for the increased proportion of SOX10-medium cells evident in Fig 3C.

Fibrinogen signalling via the BMP pathway

To determine if BMP pathway was activated throughout the OL lineage in response to fibrinogen, we measured the activation of a downstream signalling factor, SMAD1/5/9 [35]. Nuclear localization of pSMAD, as opposed to cytoplasmic, indicates activation. Using widefield microscopy in mature OLs, we observed a significant ($p < 0.05$, t-test) increase in nuclear localization of phosphorylated SMAD1/5/9 in response to fibrinogen (Fig. 4A-B) in comparison to untreated cells. Using the same microscopy, we could not convincingly detect strong signal of phosphorylated SMAD in O4+ cells in the iPSC-derived cultures. To confirm pathway activation earlier in the OL lineage, human iPSC derived OPCs were exposed to fibrinogen in the same manner and imaged by confocal microscopy. As illustrated in Fig. 4C, we detected increased signalling in the fibrinogen-treated cells in comparison to the untreated controls. Comparing the iPSC-derived cells and the primary cells (Fig. 4E), nuclear pSMAD localization was more frequent in the latter, indicating that the BMP pathway is more activated in these cells than iPSC-derived cells after exposure to fibrinogen For both primary adult and iPSC-derived O4+ cells, BMP4 treatment induced similar changes and fibrinogen-induced responses were significantly reduced by the BMP-pathway inhibitor, DHM1 ($p < 0.05$, t-test) (Fig. 4).

Bulk RNA seq analyses of fibrinogen-treated mature OLs confirmed activation of the BMP pathway (Fig. 5A), as well as an array of BMP-regulated genes (Fig 5C-D). Analysis was based on paired samples given the diversity between donors. As regards to the early OL-lineage cells, we detected a non-significant but decreasing trend in BMP pathway enrichment (Fig 5B); however, we did not observe significant changes in BMP regulated genes including those of the astrocyte lineage (data not shown). The early OL-lineage cells which were sequenced showed an overall gene suppression except for increase in cell proliferation related pathways (Fig. 3H-I).

OLs in the MS brain parallel the response seen *in vitro*

Mature oligodendrocytes identified in a publicly available RNAseq dataset from MS and control brains[32] were explored to determine if our in vitro responses could be paralleled (Fig 6A-C). Following re-clustering of the OLs, six sub-clusters were labelled Olig1-6, containing cells from both MS and non-neurologically diseased control samples. To explore BMP-pathway related signatures, each OL cluster was evaluated on the expression of top 107 target genes for the BMP4 ligand (Fig 6D). OL clusters 2-6 had more BMP genes expressed in cells derived from MS tissue rather than control. Distribution of known BMP-target genes *ID1* and *ID3* were evaluated and found to have an increasing trend in the cells derived from MS tissue (Fig 6E). To parallel this response to the signature found in our fibrinogen-treated adult OLs, the expression of lipid-related genes *ACAT2* and *MVD* was explored and found to have a similar increased trend in MS-derived samples (Fig 6F).

4. Discussion

Fibrinogen, a blood coagulation protein, is deposited in many CNS diseases with BBB disruption and myelin abnormalities, including MS, stroke and traumatic brain injury [36]. Its importance throughout the MS disease course are highlighted as BBB disruption and fibrin deposition occur early in MS lesions and precede demyelination [37], while in progressive MS cases with severe cortical fibrinogen deposition have perturbed fibrinolysis and reduced neuronal density [11].

Fibrinogen has been noted to have a functional effect on immune cells, and resident CNS glia such as astrocytes and microglia [36, 38, 39]. This molecule has been tested on rodent OPCs and OLs [17], but, to our knowledge, no studies have documented a fibrinogen effect on OL-lineage cells in human samples. Therefore, we aimed to determine if fibrinogen localizes to OL-lineage cells within the MS brain and test its functional effects on human cells *in vitro.* Here we demonstrate that fibrinogen co-localizes with OL-lineage cells (SOX10+) in the MS brain. Fibrinogen was not only localized on SOX10+ cells in MS lesions, but also in MS NAWM as well as ALS tissue.

The mature OL plays important roles in myelin maintenance and can even contribute to re-myelination in the post-natal brain [40]. To assess the functional effects of fibrinogen on OLs in relation to their stage in the cell lineage, we obtained mature human OLs from surgical resected materials as described previously[18, 19]. These samples were characterized further into late progenitors (A2B5+) and mature OLs (A2B5-) both from pediatric and adult donors. Our functional studies indicate a differential effect of fibrinogen in relation to OL lineage stage. Mature OLs (A2B5-), most apparent with adult donor cells, had increased ensheathment capacity following fibrinogen exposure, whereas fibrinogen had detrimental effects on ensheathment capacity of pediatric A2B5+ cells. Bulk RNAseq supported these positive observed effects in adult cells, showing enrichment for lipid metabolism pathways as would be upregulated in OL-mediated ensheathment and subsequent remyelination[41, 42]. Pediatric and adult human OL-lineage cells differ on a transcriptomic level, with the indication that pediatric cells are more progenitor-like [20]. These results indicate that both donor age and lineage stage underlie functional differences.

As our primary cell isolation technique is not conducive to isolation of early lineage cells (PDGFRα+ A2B5+ O4+), we derived OPCs from human iPSCs based on a recently published protocol and employed a previously characterized iPSC reporter line (SOX10mO) to aid in

determining the overall culture maturation stage [21]. We found reduced O4+ cells when fibrinogen was added during the last four days of differentiation, in line with previous rodent studies [17]. This data is further compatible with the inhibition of ensheathment by pediatric A2B5+ cells, the most progenitor-like cells within our primary cell isolates. Using the SOX10mO line, we observed an increase in the reporter-medium intensity group. We relate this finding to increased proliferation in response to fibrinogen, as shown by Ki67 and bulk RNAseq, which matches the data observed in rodent OPCs[17]. The decrease in proportion of O4+ cells was associated with the increase in cells co-expressing the astrocyte surface marker, CD49f. This deviation towards the astrocyte lineage parallels with the findings of Petersen et al.[17], although was not evident in our bulk RNAseq data. This may be due to this being a small sub-population of cells less prominent within the larger SOX10-medium sample, where overall cell cycling genes were more predominantly upregulated.

The work of the Akassoglou group determined that the effects of fibrinogen on OL-lineage cells are mediated by signaling via the BMP pathway. Using postnatal rat O4-selected cells[17] , they showed OPC differentiation was directed towards the astrocyte lineage in response to fibrinogen and confirmed this with a knockout model of the BMP type-1 receptor molecule, activin A receptor type I (ACVR1). Our analysis of this pathway indicates significant differences between the primary and the iPSC-derived OL-lineage cells. Using immunocytochemistry, we observed a strong nuclear translocation of the downstream BMP effector molecules, phosphorylated SMAD 1/5/9, in mature OLs; this response was less marked in the iPSC-derived cells. For both groups, we showed fibrinogen signaling inhibition using the ACVR1 inhibitor DMH1, showing there is some functional signaling. Our RNAseq data provides insight into the basis of the observed functional responses. Extensive gene upregulation downstream of the BMP pathway was observed in the adult primary OLs, which was paralleled in a subset of OLs from an MS RNAseq dataset and coincided with upregulation of lipid synthesis pathways in both data sources. On the other hand, the RNAseq on early OL-lineage cells showed a downregulation of all signaling pathways in response to fibrinogen, and as a result there was no enrichment for BMP pathway associated genes.

As our results have shown, the effects of BMP pathway activation are highly context dependent. In the perspective of development, studies have determined that BMP signaling has different effects dependent on developmental stage such as promoting neural progenitor cells to proliferate in early development while promoting astrocytic and neuronal differentiation in later stages[43]. These previous findings in the literature may suggest a reason for our observed age-related effect of fibrinogen in human primary OLs. As seen in our iPSC-OPCs, BMP4 signaling also has the capacity to retain cells in a progenitor-like state[44], and promotes a subset of cells to gain an astrocytic phenotype. These differences observed can be attributed to ligand and receptor availability, as well as the presence of competing signaling molecules[45].

In the context of MS, the fibrinogen-driven increased ensheathment by mature OLs could positively contribute to the remyelination process that occurs during early inflammatory demyelinating activity with ongoing breakdown of the BBB, and at the borders of chronic active plaques. In these latter situations numbers of mature OLs are relatively preserved. Failure of subsequent remyelination would reflect a depletion of such cells, as evident in previously demyelinated regions of the plaque, that is not replenished by production of new OLs capable of remyelination due a block in oligodendroglial progenitor differentiation. This could reflect at least

in part the effect of fibrinogen on OPCs. Whether other factors in the milieu of the MS lesion contribute to this differentiation block remains to be determined.

Our work was focused on MS, where fibrinogen is thought to have an important role in neuroinflammation[16, 46] and the pathogenesis of MS [15, 36, 47, 48, 49]. However, the findings could be relevant to other diseases with BBB or blood-CSF barrier breakdown (such as primary and secondary CNS tumors, infarcts, hemorrhages, trauma and infectious processes, to mention but a few) and even neurodegenerative conditions, such as Alzheimer's disease, Parkinson's disease, Huntington's disease and ALS, where fibrinogen has been found to be deposited in the CNS and has been thought to be important in their pathogenesis [50]. In this regard, we noted the deposition of fibrinogen on oligodendroglia in an ALS case included as a non-MS case in this study. Thus, fibrinogen oligodendroglial effects may have significant implications in many degenerative and non-degenerative disorders of the CNS in addition to MS.

Acknowledgements: We thank lab members Lama Fawaz, Vanessa Omana, Wolfgang Reintsch, Andrea Krahn, and Genevieve Dorval for technical or administrative assistance. The flow cytometry work and cell sorting were performed at the MNI's Early Drug Discovery Unit's Flow Cytometry Core Facility. We acknowledge the McGill microscopy platform for their support.

This project was supported in part by a grant from MS Canada.

Author Contributions: G.J.B, Q.L.C., C.W., J.P.A and G.R.W.M. contributed substantially to the conception and design of the study. G.J.B, J.P.A., G.R.W.M. and A.M. drafted a significant portion of the manuscript or figures. G.J.B., Q.L.C., C.W., A.G., A.M.R.G., C.P., A.T., M.Y., J.S., V.E.C.P., J.A.H., R.W.R.D., M.S., S.E.J.Z., W.K., S.L., A.P., T.M.D., J.A.S. contributed to acquisition and analysis of data.

Potential conflicts of interest: N/A

Data Availability:

References:

1. Bar-Or A, Li R. Cellular immunology of relapsing multiple sclerosis: interactions, checks, and balances. Lancet Neurol. 2021;20(6):470-83.
2. Rodriguez M, Scheithauer B. Ultrastructure of multiple sclerosis. Ultrastruct Pathol. 1994;18(1-2):3-13.
3. Healy LM, Stratton JA, Kuhlmann T, Antel J. The role of glial cells in multiple sclerosis disease progression. Nat Rev Neurol. 2022;18(4):237-48.
4. Cui QL, Kuhlmann T, Miron VE, Leong SY, Fang J, Gris P, et al. Oligodendrocyte progenitor cell susceptibility to injury in multiple sclerosis. Am J Pathol. 2013;183(2):516-25.
5. Kuhlmann T, Miron V, Cui Q, Wegner C, Antel J, Brück W. Differentiation block of oligodendroglial progenitor cells as a cause for remyelination failure in chronic multiple sclerosis. Brain. 2008;131(Pt 7):1749-58.
6. Zierfuss B, Larochelle C, Prat A. Blood-brain barrier dysfunction in multiple sclerosis: causes, consequences, and potential effects of therapies. Lancet Neurol. 2024;23(1):95-109.

7. Budzynski AZ. Fibrinogen and fibrin: biochemistry and pathophysiology. Crit Rev Oncol Hematol. 1986;6(2):97-146.
8. Mosesson MW. Fibrinogen and fibrin structure and functions. J Thromb Haemost. 2005;3(8):1894-904.
9. Lee NJ, Ha SK, Sati P, Absinta M, Luciano NJ, Lefeuvre JA, et al. Spatiotemporal distribution of fibrinogen in marmoset and human inflammatory demyelination. Brain. 2018;141(6):1637-49.
10. Vos CM, Geurts JJ, Montagne L, van Haastert ES, Bö L, van der Valk P, et al. Blood-brain barrier alterations in both focal and diffuse abnormalities on postmortem MRI in multiple sclerosis. Neurobiol Dis. 2005;20(3):953-60.
11. Yates RL, Esiri MM, Palace J, Jacobs B, Perera R, DeLuca GC. Fibrin(ogen) and neurodegeneration in the progressive multiple sclerosis cortex. Ann Neurol. 2017;82(2):259-70.
12. Kwon EE, Prineas JW. Blood-brain barrier abnormalities in longstanding multiple sclerosis lesions. An immunohistochemical study. J Neuropathol Exp Neurol. 1994;53(6):625-36.
13. Kirk J, Plumb J, Mirakhur M, McQuaid S. Tight junctional abnormality in multiple sclerosis white matter affects all calibres of vessel and is associated with blood-brain barrier leakage and active demyelination. J Pathol. 2003;201(2):319-27.
14. Çiçekli E, Sayan S, Kotan D. Availability of Fibrinogen/Albumin ratio in MS attack. Mult Scler Relat Disord. 2022;60:103674.
15. Ziliotto N, Bernardi F, Jakimovski D, Zivadinov R. Coagulation Pathways in Neurological Diseases: Multiple Sclerosis. Front Neurol. 2019;10:409.
16. Ryu JK, Petersen MA, Murray SG, Baeten KM, Meyer-Franke A, Chan JP, et al. Blood coagulation protein fibrinogen promotes autoimmunity and demyelination via chemokine release and antigen presentation. Nat Commun. 2015;6:8164.
17. Petersen MA, Ryu JK, Chang KJ, Etxeberria A, Bardehle S, Mendiola AS, et al. Fibrinogen Activates BMP Signaling in Oligodendrocyte Progenitor Cells and Inhibits Remyelination after Vascular Damage. Neuron. 2017;96(5):1003-12.e7.
18. Ruffini F, Arbour N, Blain M, Olivier A, Antel JP. Distinctive properties of human adult brain-derived myelin progenitor cells. Am J Pathol. 2004;165(6):2167-75.
19. Esmonde-White C, Yaqubi M, Bilodeau PA, Cui QL, Pernin F, Larochelle C, et al. Distinct Function-Related Molecular Profile of Adult Human A2B5-Positive Pre-Oligodendrocytes Versus Mature Oligodendrocytes. J Neuropathol Exp Neurol. 2019;78(6):468-79.
20. Luo JXX, Cui QL, Yaqubi M, Hall JA, Dudley R, Srour M, et al. Human Oligodendrocyte Myelination Potential; Relation to Age and Differentiation. Ann Neurol. 2022;91(2):178-91.
21. Piscopo VEC, Chapleau A, Blaszczyk GJ, Sirois J, You Z, Soubannier V, et al. The use of a SOX10 reporter toward ameliorating oligodendrocyte lineage differentiation from human induced pluripotent stem cells. Glia. 2024;72(6):1165-82.
22. Polman CH, Reingold SC, Banwell B, Clanet M, Cohen JA, Filippi M, et al. Diagnostic criteria for multiple sclerosis: 2010 revisions to the McDonald criteria. Ann Neurol. 2011;69(2):292-302.
23. Kuhlmann T, Ludwin S, Prat A, Antel J, Brück W, Lassmann H. An updated histological classification system for multiple sclerosis lesions. Acta Neuropathol. 2017;133(1):13-24.
24. Dhaeze T, Tremblay L, Lachance C, Peelen E, Zandee S, Grasmuck C, et al. CD70 defines a subset of proinflammatory and CNS-pathogenic T(H)1/T(H)17 lymphocytes and is overexpressed in multiple sclerosis. Cell Mol Immunol. 2019;16(7):652-65.

25. Broux B, Zandee S, Gowing E, Charabati M, Lécuyer MA, Tastet O, et al. Interleukin-26, preferentially produced by T(H)17 lymphocytes, regulates CNS barrier function. Neurol Neuroimmunol Neuroinflamm. 2020;7(6).
26. Bankhead P, Loughrey MB, Fernández JA, Dombrowski Y, McArt DG, Dunne PD, et al. QuPath: Open source software for digital pathology image analysis. Scientific Reports. 2017;7(1):16878.
27. Mohammadnia A, Cui Q-L, Weng C, Yaqubi M, Fernandes MGF, Hall JA, et al. Age-dependent effects of metformin on human oligodendrocyte lineage cell ensheathment capacity. Brain Communications. 2024;6(2).
28. Pernin F, Cui Q-L, Mohammadnia A, Fernandes MGF, Hall JA, Srour M, et al. Regulation of stress granule formation in human oligodendrocytes. Nature Communications. 2024;15(1):1524.
29. Love MI, Huber W, Anders S. Moderated estimation of fold change and dispersion for RNA-seq data with DESeq2. Genome Biology. 2014;15(12):550.
30. Reich M, Liefeld T, Gould J, Lerner J, Tamayo P, Mesirov JP. GenePattern 2.0. Nature Genetics. 2006;38(5):500-1.
31. Browaeys R, Saelens W, Saeys Y. NicheNet: modeling intercellular communication by linking ligands to target genes. Nature Methods. 2020;17(2):159-62.
32. Jäkel S, Agirre E, Mendanha Falcão A, van Bruggen D, Lee KW, Knuesel I, et al. Altered human oligodendrocyte heterogeneity in multiple sclerosis. Nature. 2019;566(7745):543-7.
33. Kuhlbrodt K, Herbarth B, Sock E, Hermans-Borgmeyer I, Wegner M. Sox10, a novel transcriptional modulator in glial cells. J Neurosci. 1998;18(1):237-50.
34. Barbar L, Jain T, Zimmer M, Kruglikov I, Sadick JS, Wang M, et al. CD49f Is a Novel Marker of Functional and Reactive Human iPSC-Derived Astrocytes. Neuron. 2020;107(3):436-53.e12.
35. Heldin CH, Miyazono K, ten Dijke P. TGF-beta signalling from cell membrane to nucleus through SMAD proteins. Nature. 1997;390(6659):465-71.
36. Petersen MA, Ryu JK, Akassoglou K. Fibrinogen in neurological diseases: mechanisms, imaging and therapeutics. Nat Rev Neurosci. 2018;19(5):283-301.
37. Marik C, Felts PA, Bauer J, Lassmann H, Smith KJ. Lesion genesis in a subset of patients with multiple sclerosis: a role for innate immunity? Brain. 2007;130(11):2800-15.
38. Adams RA, Bauer J, Flick MJ, Sikorski SL, Nuriel T, Lassmann H, et al. The fibrin-derived gamma377-395 peptide inhibits microglia activation and suppresses relapsing paralysis in central nervous system autoimmune disease. J Exp Med. 2007;204(3):571-82.
39. Schachtrup C, Ryu JK, Helmrick MJ, Vagena E, Galanakis DK, Degen JL, et al. Fibrinogen triggers astrocyte scar formation by promoting the availability of active TGF-beta after vascular damage. J Neurosci. 2010;30(17):5843-54.
40. Yeung MS, Zdunek S, Bergmann O, Bernard S, Salehpour M, Alkass K, et al. Dynamics of oligodendrocyte generation and myelination in the human brain. Cell. 2014;159(4):766-74.
41. Szuchet S, Yim SH, Monsma S. Lipid metabolism of isolated oligodendrocytes maintained in long-term culture mimics events associated with myelinogenesis. Proc Natl Acad Sci U S A. 1983;80(22):7019-23.
42. O'Brien JS, Sampson EL. Lipid composition of the normal human brain: gray matter, white matter, and myelin. J Lipid Res. 1965;6(4):537-44.
43. Wang RN, Green J, Wang Z, Deng Y, Qiao M, Peabody M, et al. Bone Morphogenetic Protein (BMP) signaling in development and human diseases. Genes Dis. 2014;1(1):87-105.

44. Zhang J, Fei T, Li Z, Zhu G, Wang L, Chen YG. BMP induces cochlin expression to facilitate self-renewal and suppress neural differentiation of mouse embryonic stem cells. J Biol Chem. 2013;288(12):8053-60.
45. Klumpe HE, Langley MA, Linton JM, Su CJ, Antebi YE, Elowitz MB. The context-dependent, combinatorial logic of BMP signaling. Cell Systems. 2022;13(5):388-407.e10.
46. Bardehle S, Rafalski VA, Akassoglou K. Breaking boundaries-coagulation and fibrinolysis at the neurovascular interface. Front Cell Neurosci. 2015;9:354.
47. Davalos D, Mahajan KR, Trapp BD. Brain fibrinogen deposition plays a key role in MS pathophysiology - Yes. Mult Scler. 2019;25(11):1434-5.
48. Ahmad U, Frederiksen JL. Fibrinogen: A potential biomarker for predicting disease severity in multiple sclerosis. Mult Scler Relat Disord. 2020;46:102509.
49. Alruwaili M, Al-Kuraishy HM, Alexiou A, Papadakis M, BM AL, Elhussieny O, et al. Pathogenic Role of Fibrinogen in the Neuropathology of Multiple Sclerosis: A Tale of Sorrows and Fears. Neurochem Res. 2023;48(11):3255-69.
50. Wen T, Zhang Z. Cellular mechanisms of fibrin (ogen): insight from neurodegenerative diseases. Front Neurosci. 2023;17:1197094.

Figure Legends:

Figure 1. Deposition of fibrinogen on oligodendroglial lineage cells within the MS brain.

A. Representative images of the MS plaques and MS NAWM, and ALS white matter. Sox10 (oligodendroglial marker) in green; fibrinogen in red. For each region, a higher magnification of the area within the box is shown in the panel immediately to the right. Plaque 1, an MS lesion that in sections stained for myelin showed active demyelination at its edge, consistent with a chronic active plaque; Plaque 2, an MS lesion that in sections stained for myelin showed no active ongoing demyelination, consistent with a chronic inactive plaque. Plaque 3, an MS lesion that in sections stained for myelin showed active demyelination throughout its extent, consistent with an active plaque. The representative NAWM illustrated is adjacent to Plaque 3, and the ALS white matter serves as a non-MS condition. Note the variable distribution of fibrinogen on SOX10+ cells in the MS plaques, MS NAWM and ALS white matter. Examples of fibrinogen-positive SOX10-positive oligodendroglia are indicated with white arrows. The blue arrow indicates a prominent fibrinogen-positive cell, possibly an astrocyte. Scale bars = 50µm. **B.** Quantification of the percentages of SOX10+ oligodendroglia that are positive for fibrinogen from the three MS plaques, in comparison to NAWM from the same tissue section, and from ALS white matter illustrated in A, verifying the variability of the number of fibrinogen-positive oligodendroglia.

Figure 2. Fibrinogen has an age and maturation-dependent effect on human OLs.

A. Cell viability of human A2B5+ pre-OLs (A+) and A2B5- mature OLs (A-) from adult sources following fibrinogen (Fib) treatment and quantified following immunofluorescence microscopy for propidium iodide (PI). 1:1= 4 mg/ml 1:2= 2 mg/ml 1:10= 0.4 mg/ml 1:50= 80 ug/ml. No increases in cell death were observed. **B-C.** Capacity of (B) adult (26 - 65 years) and (C) pediatric (2.5 -18 years) pre-OLs (A2B5+) (A+) and mature OLs (A2B5-) (A-) to ensheath poly-L lactide fibers. Note the increase of ensheathment capacity in adult A- cells, and the decrease in pediatric A+ cells. * $p < 0.05$, ** $p<0.01$, *** $p<0.001$. Bars indicate SEM. **D-E.** Correlation of (D) A2B5+ and (E) A2B5- cell ensheathment capacity to age, as normalized to age-matched controls following treatment with fibrinogen. Note the increasing trend in ensheathment capacity with age. **F.** Representative images of adult OLs on poly-L-lactide fibers. O4 stain in white, nuclei in blue. Top panels represent A2B5+ cells, bottom panels represent A2B5- cells. Arrows point to representative examples of focal ensheathment of the nanofibres. **G.** GO term analysis following bulk RNA sequencing on adult OL samples. **H.** Significantly upregulated genes involved in lipid metabolism, following fibrinogen treatment on adult OL samples (matched donors).

Figure 3. Fibrinogen effect on human iPSC-derived OPCs.

A. Cell viability of OPCs (O4+) imaged and quantified following immunofluorescence microscopy for propidium iodide (PI). NG: no glucose. Bars indicate SEM. **B.** Proportion of OPCs (O4+) as quantified following immunofluorescence microscopy, showing a decrease in OPCs following fibrinogen treatment for 4 days. Bars indicate SEM. * $p < 0.05$ **C.** Proportions (%) of iPSC-derived cultures expressing the mOrange reporter as measured by flow cytometry, average of n=5 passages. **D.** Proportions of cells co-expressing OPC/astrocyte markers as measured by flow cytometry. Values normalized to the average of the untreated control, n=3 passages. Bars indicate SEM. **E.** Gating technique. **G.** Differentially expressed genes following bulk RNAseq analysis of sorted reporter-medium cells. **H-I.** GO term analysis of (H) upregulated and (I) downregulated genes.

Figure 4. Fibrinogen activates BMP signalling across the OL lineage.
A. Representative images of human primary OLs (O4+) following exposure to treatments for 2 hours, by Zeiss epifluoresence microscope. **B**. Quantification of nuclear fluorescence intensity of pSMAD 1/5/9, where fibrinogen and BMP4 significantly increase pSMAD1/5/9 nuclear signal intensity. **C.** Representative images of human iPSC-derived OPCs (O4+) following exposure to treatments for 2 hours, by Zeiss confocal microscope. **D.** Quantification of nuclear fluorescence intensity of pSMAD 1/5/9 where fibrinogen and BMP4 significantly increase pSMAD1/5/9 nuclear signal intensity. **E.** Proportion of pSMAD signal localization following treatment with fibrinogen. n=3 donors for primary cells, n=4 passages for iPSC * $p < 0.05$, ** $p<0.01$, *** $p<0.001$. Bars indicate SEM.

Figure 5. Transcriptomic analysis of BMP signaling activation in the oligodendrocyte lineage.
(A-B) Single-sample Gene Set Enrichment Analysis (ssGSEA) for BMP4 target genes in: (A) human primary oligodendrocytes and (B) iPSC-differentiated SOX10-positive medium cells treated with fibrinogen (2.5 mg/mL, 4 days). Normalized read counts were used for both analyses. Enrichment scores are visualized in the bar plots. (C) Bar plot showing log2-transformed fold changes (ratios) of BMP4 target gene expression in human primary oligodendrocytes. Red bars indicate genes with higher expression levels in fibrinogen-treated cells, and blue bars indicate genes with higher expression levels in the control group. (D) Example of BMP4 target genes in human primary oligodendrocytes showing upregulation upon treatment with fibrinogen (2.5 mg/mL, 2 days). Paired t-tests were applied to assess significance levels in all plots for human primary oligodendrocytes. In all plots, blue represents control samples, and red represents fibrinogen-treated samples.

Figure 6. Transcriptomic analysis of the BMP signaling pathway in mature oligodendrocytes using single-nucleus RNA-sequencing (snRNA-seq) data.
(A) UMAP plots were generated based on the study by Jakel et al. (2019)[32] to capture all relevant cell types in the context of multiple sclerosis (MS) and control tissue. (B) Mature oligodendrocyte marker genes were used to identify mature cells within the snRNA-seq data. MOG is visualized in this UMAP plot as an example of an oligodendrocyte-specific marker gene. (C) All cell clusters contained a mixed combination of cells from MS and control patients, making them suitable for comparing BMP signaling within each oligodendrocyte population. (D) Bar plot showing the distribution of BMP4 target genes across different oligodendrocyte populations in MS and control groups. We used the top 107 target genes for the BMP4 ligand (with interaction weight > 0.1) and extracted their average expression in each oligodendrocyte cluster from both MS and control groups. The Oligo1 population was excluded because most of its cells (85%) originated from control samples. In the bar plot, purple, red, and blue represent not expressed, higher expression in MS, and higher expression in control samples, respectively. (E) ID1 and ID3 are examples of BMP signaling target genes that show an increasing trend in expression in most oligodendrocyte populations in MS compared to control groups. (F) Example of genes related to lipid metabolism that exhibit a similar increasing trend in gene expression as BMP signaling target genes, consistent with the results from in vitro experiments using human primary oligodendrocytes. In all cases, normalized read count data were used to calculate average expression levels for each cluster for analysis and plot generation. Red represents MS, and blue represents control cells.

Supplemental Data:

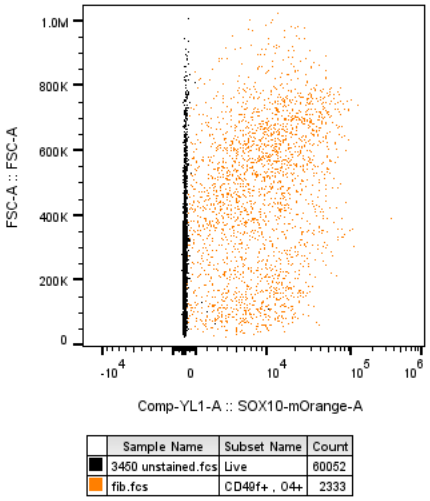

Figure S1. mOrange signal in hybrid OPCs. Following 4-day treatment of fibrinogen, data acquired by flow cytometry. CD49f+O4+ cells express mOrange (orange) at a higher fluorescence intensity than non-reporter cells (black).

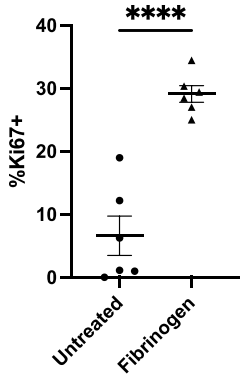

Figure S2. Proliferation in fibrinogen treated OPC cultures. Proportion of Ki67+ nuclei quantified in iPSC-OPC cultures treated with fibrinogen. $p < 0.0001$. n=6 replicates, bars indicate SEM.

Table S1. Tissue Donor information.

Section	Age (years)	Sex	Disease Type	EDSS	Disease Duration	Post-mortem interval
MS Plaque 1	48	M	SPMS	8.5	6 years	N/A
MS Plaque 2	60	F	SPMS	8.5	28 years	2.5 hrs
MS Plaque 3	44	F	RRMS	7	13 years	5 hr
ALS White Matter	78	M	ALS	N/A	3 years	16 hrs

Abbreviations: ALS=Amyotrophic Lateral Sclerosis, EDSS=Expanded Disability Status Scale, F= Female, M=Male, MS=Multiple Sclerosis, N/A=Not Available, RRMS=Relapsing-remitting MS, SPMS=Secondary Progressive MS.

Table S2. iPSC Line Information

Cell Line Name	Sex	Patient Age (years)	Material Source	Type of Reprogramming
AIW002-02	M	37	PBMC	Retrovirus
3450	M	37	PBMC	Episomal
SOX10mOrange (3450)	M	37	PBMC	Episomal

Abbreviations: M=Male, PBMC= Peripheral Blood Mononuclear Cells.

Table S3. Antibodies and Reagents

Antibody	Company	Identifier
goat anti-SOX10	R&D systems, Oakville ON	AF2864
rabbit anti-Fibrinogen	Agilent, Santa Clara CA	A0080
isotype control polyclonal rabbit	BioLegend, San Diego CA	910801
isotype control goat IgG	R&D systems, Oakville ON	AB 108-C
O4-APC	Miltenyi, Auburn CA	130-119-982
Human TruStain FcX Fc Receptor Blocking Solution	BioLegend, San Diego CA	422302
LIVE/DEAD Fixable Aqua Dead Cell Stain Kit, for 405nm excitation	Invitrogen, Waltham MA	L34957
CD49f-PE-Dazzle	BioLegend, San Diego CA	313626
mouse IgM anti-O4	R&D, Oakville ON	MAB1326
rabbit anti-pSMAD (phosphorylated Suppressor of Mothers against Decapentaplegic) 1/5/9	Cell Signalling Technology, Danvers MA	13820S
rat anti-Ki67	Invitrogen, Waltham MA	14-5698-82

IHC Staining Protocol

Frozen human brain tissue sections, previously briefly fixed in acetone, were further fixed in 100% acetone for 10 minutes, followed by 70% ethanol for 5 minutes. Subsequently, sections were washed with PBS and 0.05% PBST (phosphate-buffered saline + Tween20) for 3 minutes. Fc-receptors in sections were blocked with PBS containing 10% donkey serum. Primary antibodies, goat anti-SOX10 (R&D systems, Oakville ON, AF2864) and rabbit anti-fibrinogen (Agilent, Santa Clara CA, A0080) were diluted 1:500 (0.2 mg/ml) and 1:400 (1mg/ml) respectively in PBS containing 3% donkey serum and incubated overnight at 4°C. Isotype controls consisted of the IgG of the same species and same concentration as each primary antibody. Following incubation, sections were washed with 0.05% PBST 3 times for 5 minutes each. Fluorophore-conjugated secondary antibodies (Invitrogen, Waltham MA) were prepared at a 1:200 dilution in PBS, donkey anti-goat IgG Alexa Fluor 488 to visualize SOX10 and donkey anti-rabbit IgG Alexa Fluor 647 to visualize fibrinogen and slides were incubated in the dark for 60 minutes at room temperature. Sections were washed with 0.05% PBST 3 times for 3 minutes and incubated with Hoechst (Invitrogen, Waltham MA; 1:5000) for 10 minutes at room temperature. Once washed with 0.05% PBST 3 times for 3 minutes to block lipofuscin autofluorescence, sections were incubated with 0.3% TrueBlack (Biotium, Fremont, CA) diluted in 70% ethanol for 3 minutes. Slides were washed with PBS and mounted with PermaFluor mounting medium (Thermo-Fisher, Missisauga, ON), coverslipped and stored in the dark at 4°C.

Figure 1

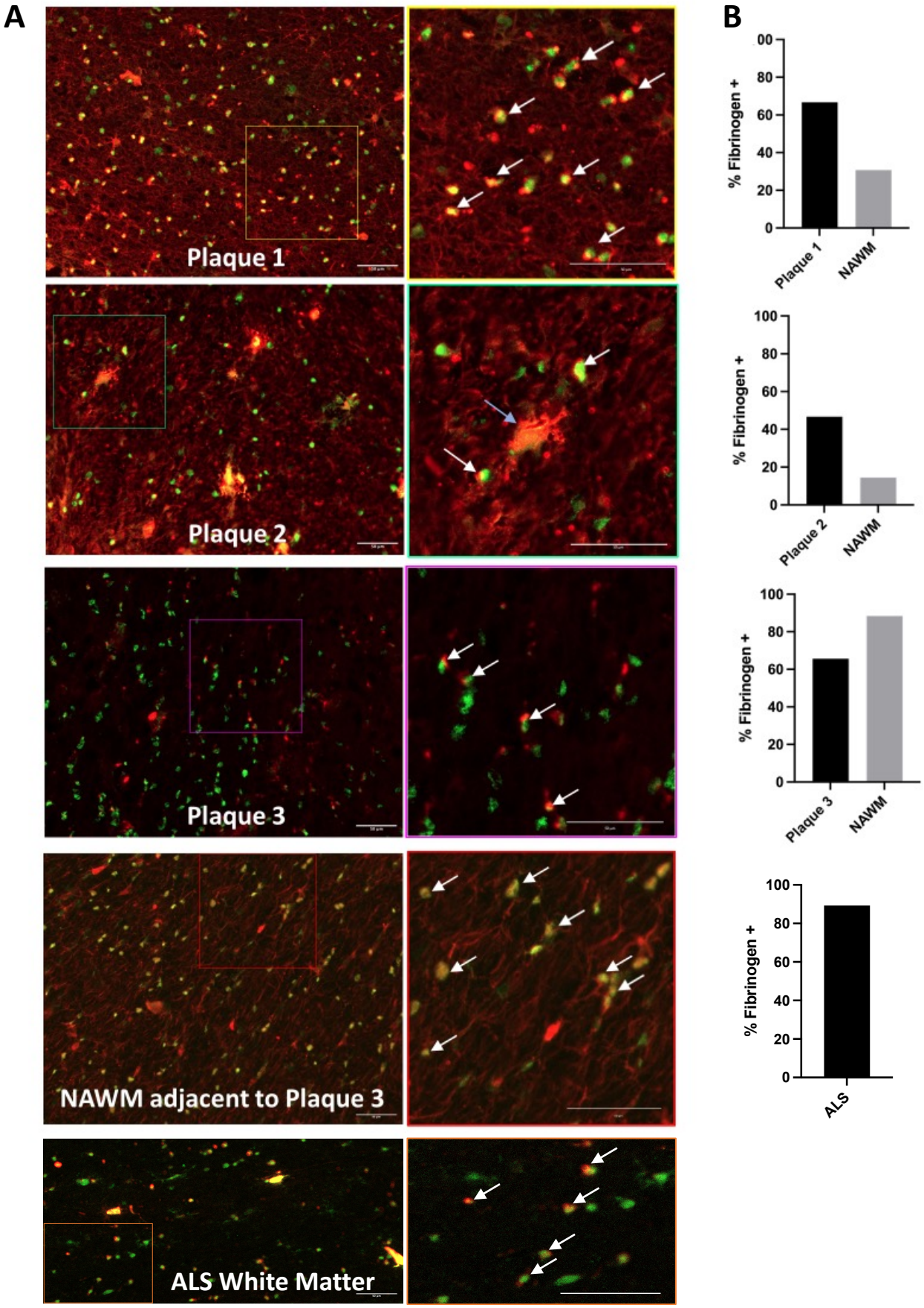
A
Plaque 1
Plaque 2
Plaque 3
NAWM adjacent to Plaque 3
ALS White Matter
B
% Fibrinogen +
0
20
40
60
80
100
Plaque 1
NAWM
Plaque 2
NAWM
Plaque 3
NAWM
ALS

Figure 2

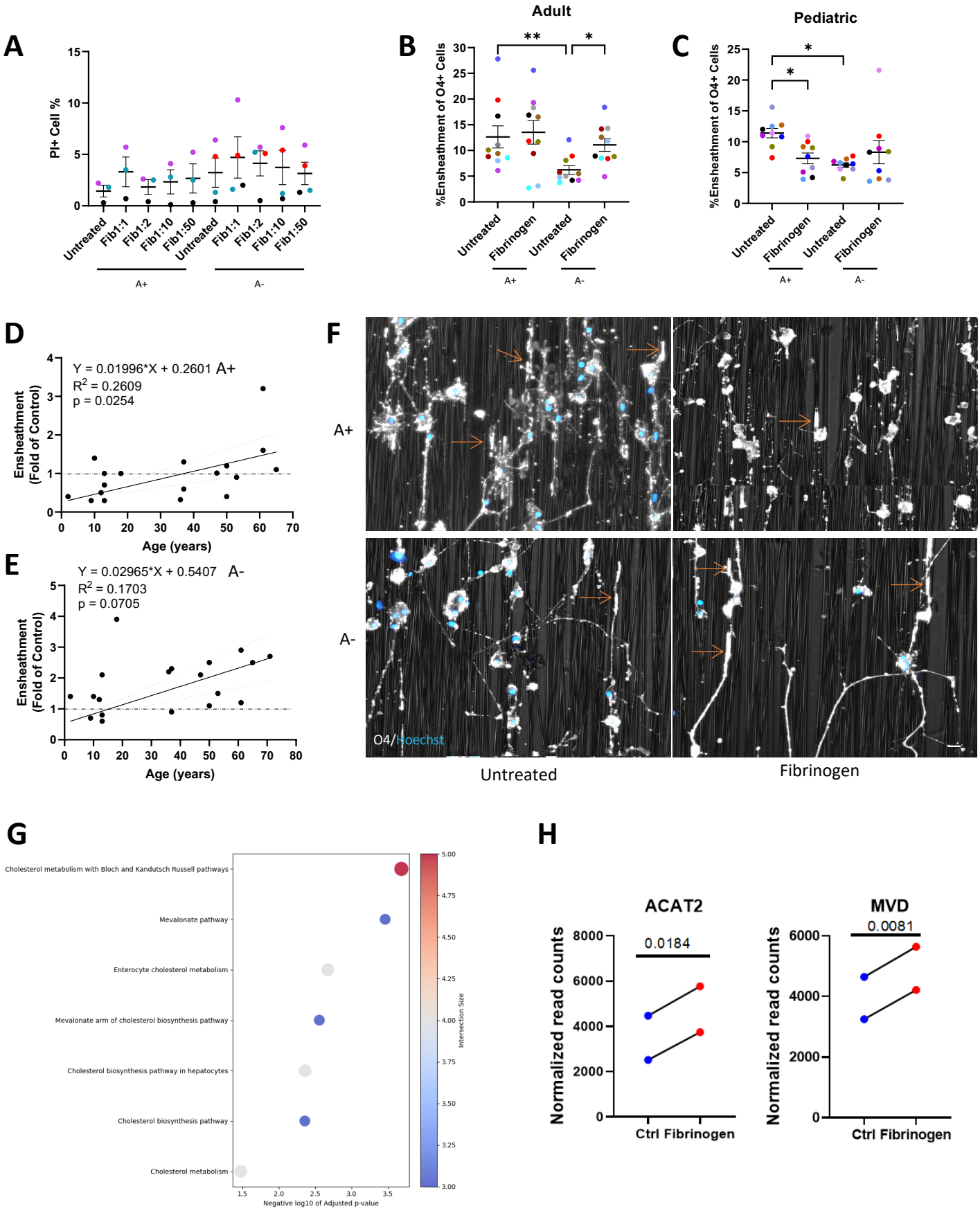
A
PI+ Cell %
Untreated
Fib1:1
Fib1:2
Fib1:10
Fib1:50
A+
A-
B
Adult
%Ensheathment of O4+ Cells
Untreated
Fibrinogen
C
Pediatric
D
Y = 0.01996*X + 0.2601 A+
R2 = 0.2609
p = 0.0254
Ensheathment (Fold of Control)
Age (years)
E
Y = 0.02965*X + 0.5407 A-
R2 = 0.1703
p = 0.0705
F
A+
A-
O4/Hoechst
Untreated
Fibrinogen
G
Cholesterol metabolism with Bloch and Kandutsch Russell pathways
Mevalonate pathway
Enterocyte cholesterol metabolism
Mevalonate arm of cholesterol biosynthesis pathway
Cholesterol biosynthesis pathway in hepatocytes
Cholesterol biosynthesis pathway
Cholesterol metabolism
Negative log10 of Adjusted p-value
Intersection Size
H
ACAT2
0.0184
MVD
0.0081
Normalized read counts
Ctrl
Fibrinogen

Figure 3

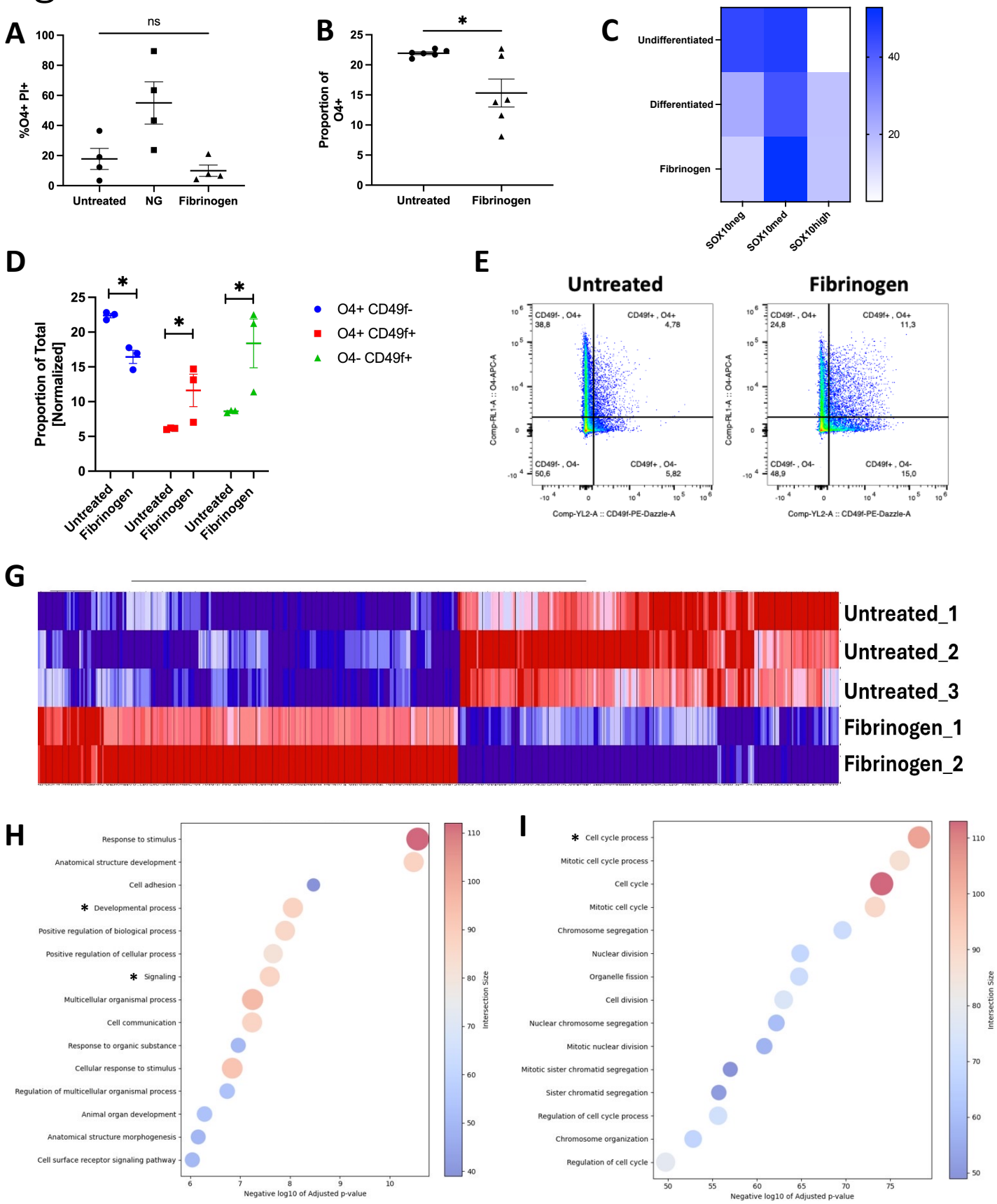
A
ns
%O4+ PI+
Untreated
NG
Fibrinogen
B
*
Proportion of O4+
Untreated
Fibrinogen
C
Undifferentiated
Differentiated
Fibrinogen
SOX10neg
SOX10med
SOX10high
D
Proportion of Total [Normalized]
O4+ CD49f-
O4+ CD49f+
O4- CD49f+
Untreated
Fibrinogen
E
Untreated
Fibrinogen
CD49f- , O4+ 38,8
CD49f+ , O4+ 4,78
CD49f- , O4- 50,6
CD49f+ , O4- 5,82
CD49f- , O4+ 24,8
CD49f+ , O4+ 11,3
CD49f- , O4- 48,9
CD49f+ , O4- 15,0
Comp-RL1-A :: O4-APC-A
Comp-YL2-A :: CD49f-PE-Dazzle-A
G
Untreated_1
Untreated_2
Untreated_3
Fibrinogen_1
Fibrinogen_2
H
Response to stimulus
Anatomical structure development
Cell adhesion
* Developmental process
Positive regulation of biological process
Positive regulation of cellular process
* Signaling
Multicellular organismal process
Cell communication
Response to organic substance
Cellular response to stimulus
Regulation of multicellular organismal process
Animal organ development
Anatomical structure morphogenesis
Cell surface receptor signaling pathway
Negative log10 of Adjusted p-value
Intersection Size
I
* Cell cycle process
Mitotic cell cycle process
Cell cycle
Mitotic cell cycle
Chromosome segregation
Nuclear division
Organelle fission
Cell division
Nuclear chromosome segregation
Mitotic nuclear division
Mitotic sister chromatid segregation
Sister chromatid segregation
Regulation of cell cycle process
Chromosome organization
Regulation of cell cycle
Negative log10 of Adjusted p-value
Intersection Size

Figure 4

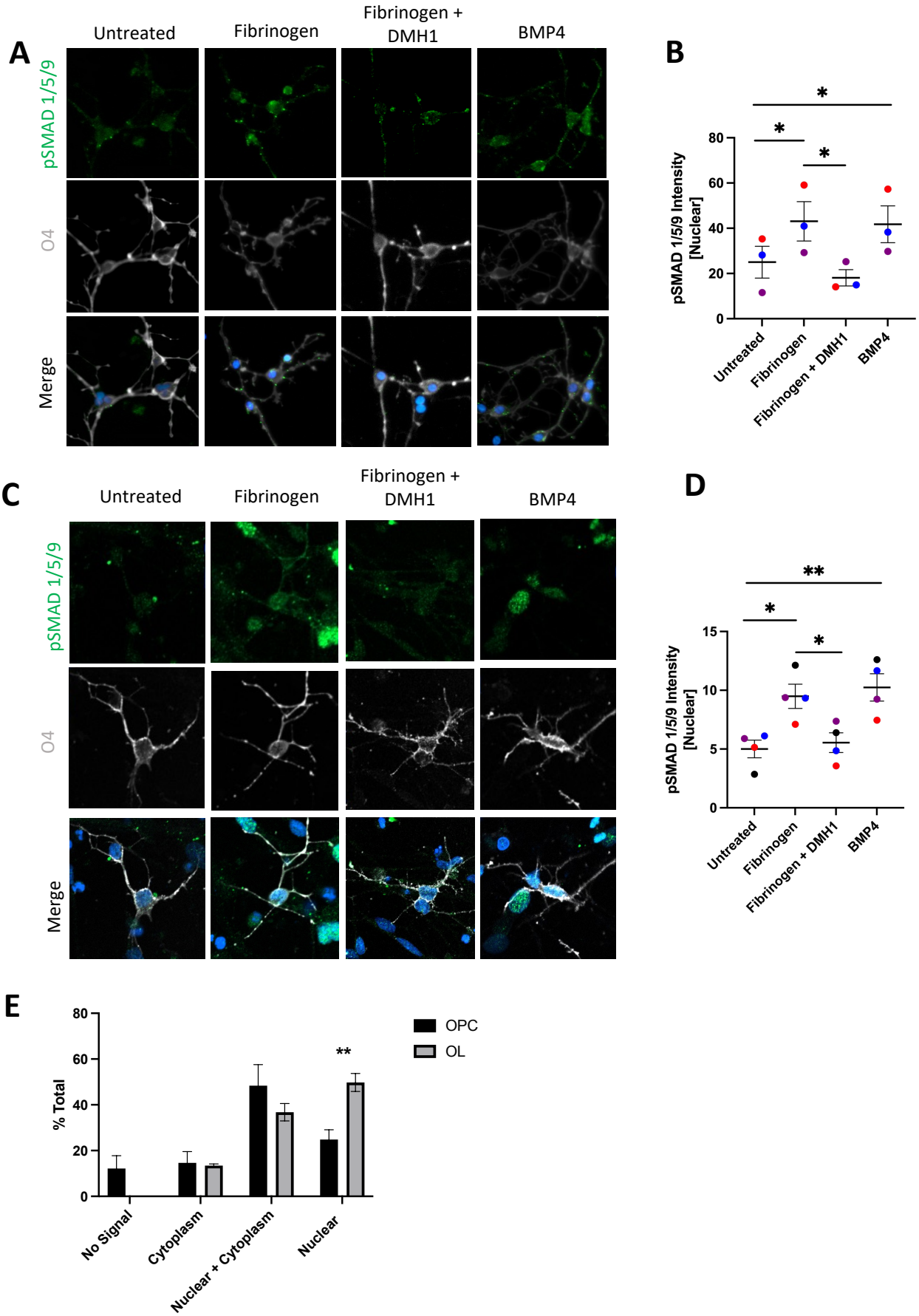
A
Untreated
Fibrinogen
Fibrinogen + DMH1
BMP4
pSMAD 1/5/9
O4
Merge
B
pSMAD 1/5/9 Intensity [Nuclear]
0
20
40
60
80
*
*
*
Untreated
Fibrinogen
Fibrinogen + DMH1
BMP4
C
Untreated
Fibrinogen
Fibrinogen + DMH1
BMP4
pSMAD 1/5/9
O4
Merge
D
pSMAD 1/5/9 Intensity [Nuclear]
0
5
10
15
**
*
*
Untreated
Fibrinogen
Fibrinogen + DMH1
BMP4
E
% Total
0
20
40
60
80
OPC
OL
**
No Signal
Cytoplasm
Nuclear + Cytoplasm
Nuclear

Figure 5

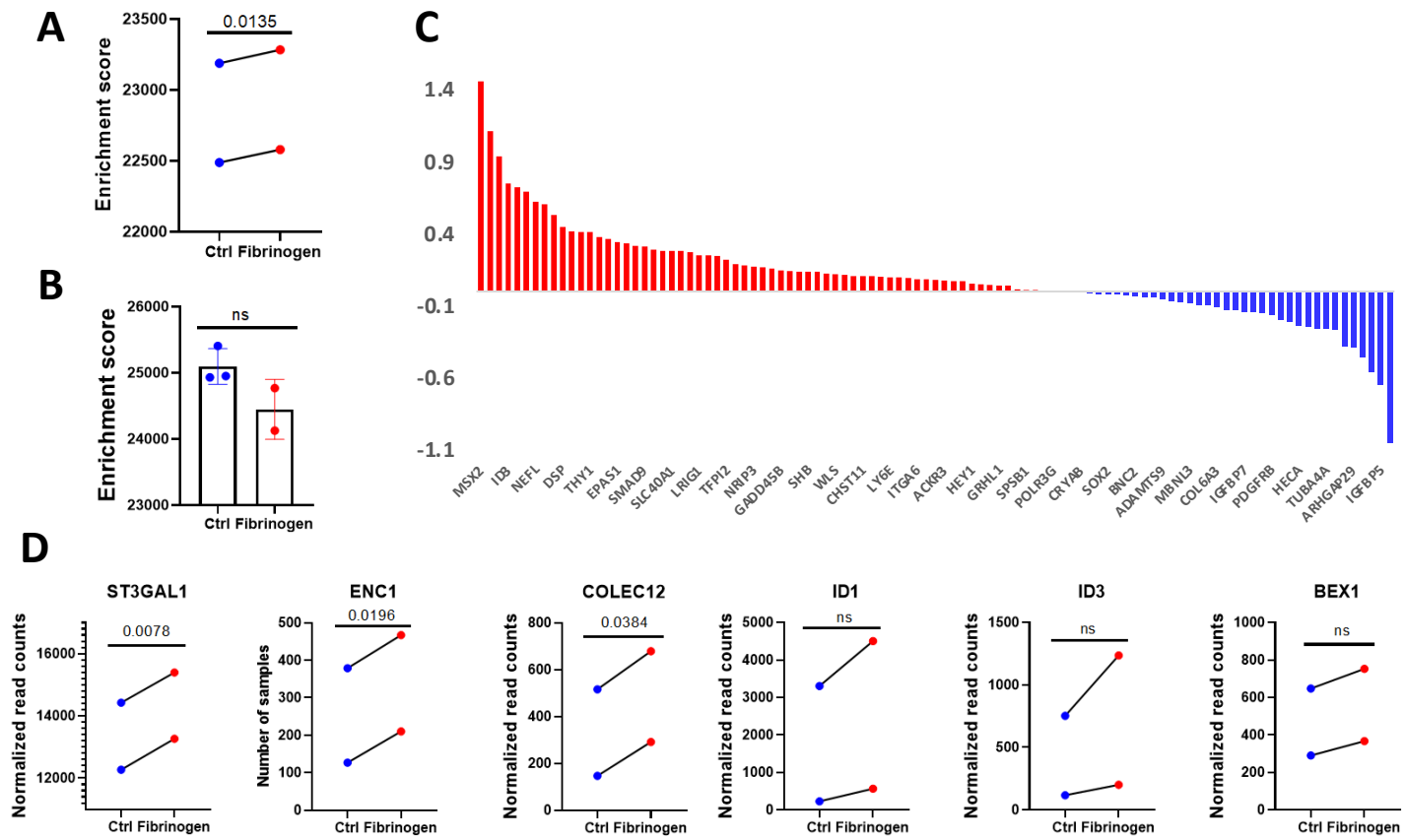
A
0.0135
Enrichment score
23500
23000
22500
22000
Ctrl Fibrinogen
B
ns
Enrichment score
26000
25000
24000
23000
Ctrl Fibrinogen
C
1.4
0.9
0.4
-0.1
-0.6
-1.1
MSX2
ID3
NEFL
DSP
THY1
EPAS1
SMAD9
SLC40A1
LRIG1
TFPI2
NRIP3
GADD45B
SHB
WLS
CHST11
LYGE
ITGA6
ACKR3
HEY1
GRHL1
SPSB1
POLR3G
CRYAB
SOX2
BNC2
ADAMTS9
MBNL3
COL6A3
IGFBP7
PDGFRB
HECA
TUBA4A
ARHGAP29
IGFBP5
D
ST3GAL1
0.0078
Normalized read counts
16000
14000
12000
Ctrl Fibrinogen
ENC1
0.0196
Number of samples
500
400
300
200
100
0
Ctrl Fibrinogen
COLEC12
0.0384
Normalized read counts
800
600
400
200
0
Ctrl Fibrinogen
ID1
ns
Normalized read counts
5000
4000
3000
2000
1000
0
Ctrl Fibrinogen
ID3
ns
Normalized read counts
1500
1000
500
0
Ctrl Fibrinogen
BEX1
ns
Normalized read counts
1000
800
600
400
200
0
Ctrl Fibrinogen

Figure 6

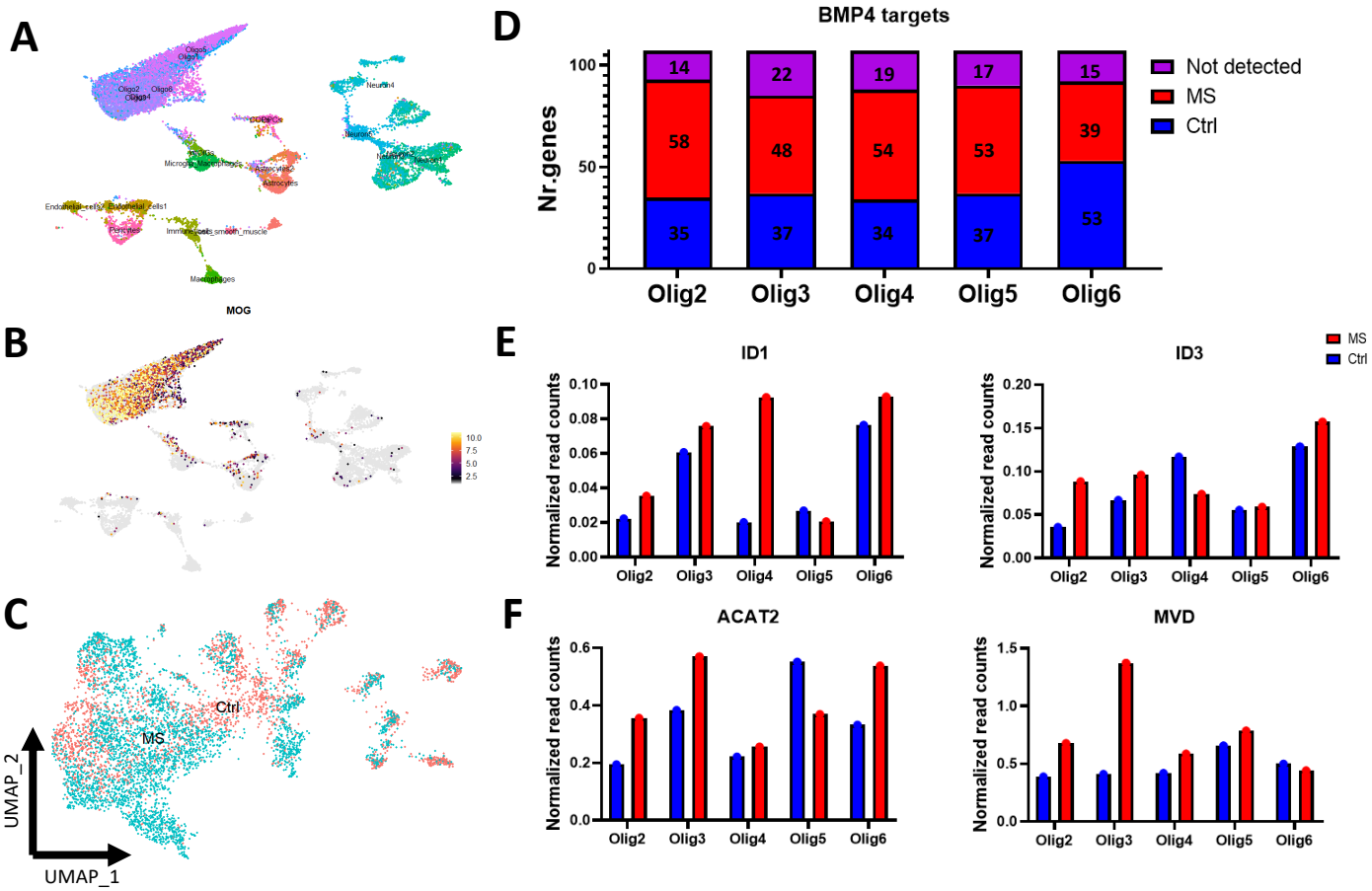
A
MOG
B
10.0
7.5
5.0
2.5
C
Ctrl
MS
UMAP_2
UMAP_1
D
BMP4 targets
Nr.genes
100
50
0
14
58
35
22
48
37
19
54
34
17
53
37
15
39
53
Olig2
Olig3
Olig4
Olig5
Olig6
Not detected
MS
Ctrl
E
ID1
ID3
Normalized read counts
0.10
0.08
0.06
0.04
0.02
0.00
0.20
0.15
0.10
0.05
0.00
Olig2
Olig3
Olig4
Olig5
Olig6
MS
Ctrl
F
ACAT2
MVD
Normalized read counts
0.6
0.4
0.2
0.0
1.5
1.0
0.5
0.0
Olig2
Olig3
Olig4
Olig5
Olig6